Optimising Connectivity-based Fixel Enhancement: A method for whole-brain statistical analysis of diffusion MRI

David Raffelt[1], Robert E Smith[1], J-Donald Tournier[2,3], Gerard R Ridgway[4,5], David Vaughan[1,6], and Alan Connelly[1,7]

[1]*Florey Institute of Neuroscience and Mental Health, Melbourne, VIC, Australia,* [2]*Centre for the Developing Brain, King's College London, London, United Kingdom,* [3]*Department of Biomedical Engineering, King's College London, London, United Kingdom,* [4]*FMRIB Centre, University of Oxford, Oxford, United Kingdom,* [5]*UCL Institute of Neurology, University College London, London, United Kingdom,* [6]*Department of Medicine, University of Melbourne, Melbourne, Australia,* [7]*The Department of Florey Neuroscience and Mental Health, University of Melbourne, Melbourne, VIC, Australia*

Target Audience: Researchers and clinicians interested in performing whole-brain multi-subject analysis of diffusion-weighted MRI (DWI).

Purpose: To optimise input parameters for a recently developed whole-brain DWI statistical method that is robust to crossing fibres.

Introduction: In the field of DWI, voxel-based analysis (VBA) is being increasingly used to study white matter development, aging and pathology. In VBA of white matter there are two issues that have been largely neglected to date:

1) Commonly used software for statistical inference cannot handle fibre population-specific quantitative measures derived from higher order models (e.g. CHARMED[1], Apparent Fibre Density (AFD)[2], HMOA[3], CUSP-MFM[4]).
2) Axons are oriented and span many voxels. Distant voxels can share the same underlying anatomy, while at the same time neighbouring voxels may share no anatomy (e.g. at a bundle interface). It is therefore reasonable to assume that correlations in quantitative measures can occur anywhere along a fibre tract, and not necessarily with all voxel neighbours isotropically.

Both issues 1 and 2 are problematic for smoothing and cluster-based inference. A neighbourhood for traditional isotropic smoothing and clustering is ambiguous when adjacent voxels have multiple fibre populations, and ill-defined when adjacent fibre populations belong to different fibre tracts. A statistical method was recently developed (Connectivity-based Fixel Enhancement, CFE[5]) that circumvents these issues by identifying a neighbourhood for each fixel (*population of fibres* within a single *voxel*[6]) using probabilistic fibre tractography. The CFE method is based on threshold-free cluster enhancement (TFCE)[7], where the test-statistic at each fixel, f, is enhanced based on the height of the test-statistic, h, and the extent, e, of the supporting sections beneath it (Eq. 1). Extending TFCE, the CFE method defines e as the weighted sum of supra-threshold fixels *structurally connected* to fixel f, as inferred by tractography (where the connectivity, c_i, is the proportion of shared streamlines between fixel f and i) (Eq. 2). The constant C enables the investigator to increase the influence of fixels connected by long range (probabilistically less likely) streamlines (with C < 1). In the CFE method, pre-smoothing is also constrained to fixels of the same tract using the connectivity-derived neighbourhood.

$$CFE(f) = \int_{h=h_0}^{h_f} e(h)^E h^H dh \qquad (1)$$

$$e(h) = \sum_{i=1}^{n} c_i^C \qquad (2)$$

The CFE method has been previously applied to investigate Alzheimer's Disease[5], Dravet's Syndrome[8], adolescence born preterm[9], and temporal lobe Epilepsy[6]. However it is not yet known what the optimal values for E, H, C and pre-smoothing are, and if they are dependent on effect size and pathology region. In this work we have assessed the performance of CFE by introducing simulated pathology into *in vivo* data. We explored combinations of E, H and C while varying the pathology region, effect size and pre-smoothing spatial extent. Performance was assessed using a receiver-operator characteristic (ROC)-based evaluation.

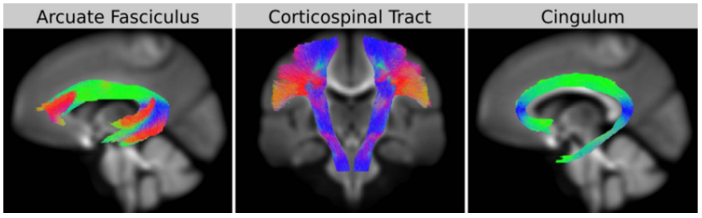

Figure 1. *Template-derived streamlines used to indicate regions-of-interest for simulating pathology. Pathology was introduced by reducing the AFD in fixels associated with these streamlines. Tracts were selected to cover a broad range of properties (crossing fibres, curvature, fanning, and width).*

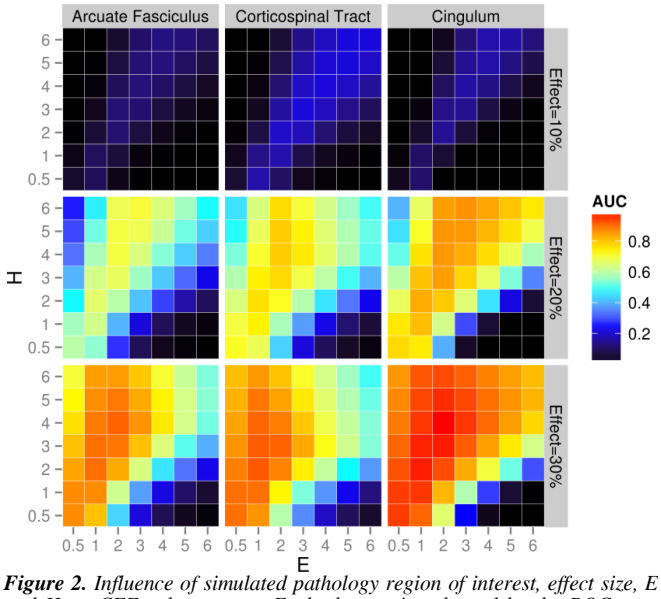

Figure 2. *Influence of simulated pathology region of interest, effect size, E and H on CFE enhancement. Each element is coloured by the ROC area under the curve (AUC). All plots were generated with C = 0 and smoothing = 10mm since these gave best results for most combinations.*

Methods: DWI were acquired from 80 healthy subjects on a 3T Siemens Trio, 60 directions, b=3000 s/mm^2, 2.3mm. Motion correction, bias field correction and intensity normalisation were performed[2]. Fibre Orientation Distributions (FODs) were computed using robust constrained spherical deconvolution[10], then registered to a study-specific FOD template[2]. Fixels common to all subjects were computed by segmenting each FOD 'lobe' in the template[11] (i.e. a fixel mask). The FOD template was used to generate 3 million streamlines with the iFOD2 tractography algorithm[12]. ROIs (arcuate fasciculus, corticospinal tract, and cingulum) were identified by extracting streamlines from the whole-brain tractogram, then mapping streamlines to fixels in the template fixel mask. Pathology was introduced into half of the subjects by reducing the AFD in ROI fixels (effect sizes 10%, 20%, and 30%). AFD data was pre-smoothed using a range of connectivity-based smoothing kernels (0, 5, 10, 20mm FWHM). To evaluate both false-positive rate (FPR) and true-positive rate (TPR), the groups were compared both before and after the addition of simulated pathology. By permuting group membership, 5000 instances of each of these "null" and "non-null" t-statistics were computed. Both null and non-null t-statistic images were enhanced using CFE with combinations of E = 0.5, 1, 2, 3, 4, 5, 6, H = 0.5, 1, 2, 3, 4, 5, 6, C = 0, 0.25, 0.5, 0.75, 1.0. As in [7], CFE performance was assessed using the alternative free-response ROC (AFROC) method, which uses a family-wise error corrected FPR computed from the enhanced noise only image. The TPR was computed as the fraction of suprathreshold ROI fixels in the enhanced signal + noise image.

Results: Shown in Fig. 2 are plots of the area under the curve (AUC) computed on the AFROC curves for FPR < 0.05. All plots were generated with C = 0, since this gave the highest AUC for all results except with 10% effect size cingulum pathology (not shown). As shown in Fig. 2, the optimal values of E and H are not heavily dependent on the pathology ROI. Effect sizes of 20% and 30% gave similar optimal values for E and H. With a lower effect size of 10%, slightly larger E values gave better results. AUC improved as smoothing was increased from 0-10mm, with no further change with 20mm smoothing (not shown).

Discussion and Conclusion: We have demonstrated that the optimal CFE parameters are relatively insensitive to pathology region and effect size. This is encouraging for future fixel-based analyses since maximum sensitivity should be obtained for most studies with H = 4 and E = 2-3. In contrast to TFCE, the optimal E value is greater than 1, and therefore enhancement increases more than linearly with extent size. This difference is likely due to the extent being constrained to related fixels by tractography-based connectivity. Note that an optimal value of C = 0 implies that better enhancement is achieved when all connected neighbourhood fixels contribute with an equal amount regardless of their probabilistic connectivity weight. While the optimal smoothing kernel of 10mm FWHM is relatively large compared to the 3mm suggested in TFCE[7], the connectivity-based smoothing ensures that minimal blurring occurs across unrelated fibre tracts and therefore such a large kernel is unlikely to decrease specificity.

References: **[1]** Assaf Y et al. (2005) NeuroImage.27(1):48-58 **[2]** Raffelt D et al (2012) Neuroimage. 15;59(4):3976-94. **[3]** Dell'Acqua F et al. (2012) Hum Brain Mapp. doi:10.1002/hbm.22080. **[4]** Scherrer B et al. PloS One. 7(11):e48232. **[5]** Raffelt D et al., Proc. ISMRM 21, 841 (2013). **[6]** Raffelt D et al., Proc. ISMRM 22, 731 (2014)**[7]** Smith S et al. (2009) Neuroimage. 1;44(1):83-98. **[8]** Raffelt D et al., Proc. ISMRM 22, 1904 (2013). **[9]** Raffelt D et al., Proc. ISMRM 22, 1755 (2013). **[10]** Tournier D et al., Proc. ISMRM 21, 0773 (2013). **[11]** Smith RE et al., Neuroimage 67, 298–312 (2013) **[12]** Tournier D et al., Proc. ISMRM 21, 0773 (2013)